Article

MMS

Mathematics and Mechanics of Solids
2024, Vol. 29(6) 1254–1270


Article reuse guidelines:
sagepub.com/journals-permissions
DOI: 10.1177/10812865231203154
journals.sagepub.com/home/mms


The mathematics and mechanics of tug of war

Derek E Moulton
Mathematical Institute, University of Oxford, Oxford, UK

Hadrien Oliveri
Mathematical Institute, University of Oxford, Oxford, UK

Received 22 May 2023; accepted 7 September 2023

Abstract

In this paper, we propose a mechanical model for a game of tug of war (rope pulling). We focus on a game opposing two players, modelling each player's body as a structure composed of straight rods that can be actuated in three different ways to generate a pulling force. We first examine the static problem of two opponents being in a deadlock configuration of mechanical equilibrium; here we show that this situation is essentially governed by the ratio of masses of the players, with the heavier player having a strong advantage. We then turn to the dynamic problem and model the response of the system to an abrupt change in activation by one of the players. In this case, the system exhibits a nontrivial response; in particular, we compare a sudden pulling and a sudden "letting up," and demonstrate the existence of regimes in which the lighter player can momentarily take the advantage.

Keywords

Tug of war, mechanics, biomechanics, sport, mathematical modelling

"The final lines are not mine: they come from an experiment on soft matter, after Boudin […]. An English translation might run like this:

Have fun on sea and land
Unhappy it is to become famous
Riches, honors, false glitters of this world
All is but soap bubbles"

Pierre-Gilles de Gennes, Nobel lecture, 1991.

Corresponding author:
Derek E Moulton, Mathematical Institute, University of Oxford, Oxford OX2 6GG, UK.
Email: moulton@maths.ox.ac.uk

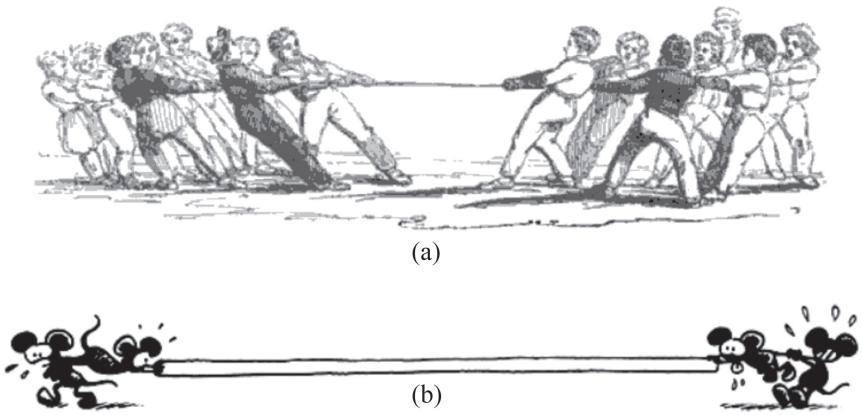

(a)

(b)

Figure 1. (a) A group of children playing tug of war. Prior to the 20th century, the game was commonly known in the anglophone world as the game of *French and English* [10, 11], likely owing to the tense historical ties between France and Britain. Drawing reproduced from Williams [10] (public domain). (b) Four little mice in a fierce tug of war. Image adapted from McMillen and Goriely [12] with presumed courtesy from Alain Goriely.

1. Introduction

Tug of war (also known as *tug o' war*, *tug war*, *rope war*, *rope pulling*, or *tugging war*) refers to "an athletic contest between two teams who haul at the opposite ends of a rope, each trying to drag the other over a line marked between them" [1]. Tug of war has a rich history and unclear origins and is arguably one of the oldest known games in humanity, played for ritual, political, military, commemorative, sportive, or recreational (1) purposes in various cultures [2–4]. Its most ancient representations can be traced back to as early as the Bronze Age[1] [5], and historical and mythological variants can be found galore, for example, in ancient Greece [6], Cambodia,[2] China [4], India,[3] Afghanistan, Japan, Korea, South America, Europe, and Togo; as well as in Inuit traditions [7] or Scandinavian legends [8]. Rope pulling is now a codified sport [9], played in all countries in the world by amateur and professional athletes.

The game's iconic power has been exemplified in popular culture, with reference in shows such as *Squid Game*, a Korean dramatic series from 2021. In a graphic metaphor for social Darwinism [13, 14], hundreds of financially cornered players compete for money in various mortal games, including a tug of war in which the weakest team is liquidated by being dragged towards a precipice. Luckily, in reality, tug of war is generally played in more companionable conditions; nonetheless, it is a physically intense and technically challenging sport that may involve huge mechanical forces. It is thus not entirely surprising that several more or less serious tug-of-war accidents have been reported [15–17], such as the dramatic Taipei incident of 1997. In a mammoth rope-pulling contest commemorating Retrocession Day, and featuring a staggering 1,600 participants, the inadequate, 2-inch thick nylon cord snapped under overwhelming tension, unleashing a devastating amount of kinetic energy. The incident resulted in injuries to 42 individuals, with two having an arm torn off,[4] and plunged the municipality into serious political-mediatic turmoil. Two years earlier, one of the worst disasters in tug of war history occurred in Germany, when 650 Boy Scouts attempted to win a place in the Guinness Book of Records. The unsuited, thumb-thick rope chosen for the event inevitably snapped, killing two young boys, and causing injuries to 102 participants.[5] Several other cases have been reported where rope snapping and/or unsafe gripping resulted in various injuries such as limb severing.[6] Notwithstanding these rare but shocking incidents, mostly caused by amateurish negligence and irresponsible underestimation of the forces at play, tug of war is overall safe, as long as the players use the right equipment and follow the rules and safety guidelines [9].

From a mechanical perspective, tug of war presents an intriguing system, seemingly simple in its complexion—forces are applied to opposing ends of a rope—but with significant complexity in its execution: the configuration of each player, many different muscle groups potentially generating forces in different ways, timing, footing, stabilisation after slipping, and so on, all play a role in the outcome of a game. In practice, teams use strategies such as the drop-step, heel-toe, sitting, bracing, quick pull, and counterbalance techniques to establish a robust foundation, emphasise footwork, maximise strength, create sudden bursts of power, and strategically position team members. These techniques contribute to the dynamic nature of tug-of-war, enabling

teams to employ diverse tactics based on their strengths and objectives. In this paper, we mathematically address a simple question: How to win a game of tug of war?

Biomechanical [18–22] and mathematical [4, 23–25] analyses of tug of war have been proposed, often focusing on the biomechanics of one player pulling on a fixed rope. Here, the focus is rather on the mechanics and dynamics of the game itself, that is, the competition between several opponents. In particular, we attempt to determine the mechanical determinants of a victory (e.g. posture, body characteristics, and strength). Therefore, we propose a mathematical model for a tug of war between two players, simple enough to enable mathematical analysis but with enough complexity and degrees of activation freedom to mimic potential strategies within a real game. We first study the static case, namely a deadlocked situation of mechanical equilibrium, and we compare each player's propensity to slip as a function of three distinct modes of pulling activation. In that case, we show that the outcome of the game is almost fully dictated by player weight, more than any other physical characteristic. We then turn to the dynamic case, in which inertial effects induced by a sudden change in activation create a rich dynamic structure, and where a lighter player may be momentarily able to make the heavier one slip or stumble.

2. Model

The setup for our model is shown schematically in Figure 2. We consider a two-player game, with the players situated in the x-y plane. We concentrate the mass of Player 1 at the point (x_1, y_1) and define their body orientation by two angles: θ_1 defines the angle of the lower body with respect to the horizontal x-axis, while ϕ_1 is the angle between the lower and upper body, due to bending at the hips. That is, a line passing through the torso and the point (x_1, y_1), which we term the "torso axis", makes angle ϕ_1 with a line passing through the lower body, which we term the "leg axis." The torso has fixed length ℓ_1^T, while the legs have length ℓ_1^L, which will vary due to the bending of the knees. The player holds the rope at a distance ℓ_1^A from the point (x_1, y_1). Similar quantities are defined for Player 2, noted with subscript 2 (Figure 2(a)). Henceforth, we denote with a superscript A, L, and T, quantities related to the *arms*, *legs*, and *torso*, respectively.

In order to incorporate independent activation of the leg and arm muscles, we idealise each player's lower body as an actuatable rod situated along the leg axis and with the arms described as a separate rod connecting the concentrated mass to the holding point of the rope via a line that is aligned with the rope. We employ the theory of morphoelastic rods [26, 27], which gives a mathematical framework for growing elastic rods, in order to describe the independent active pulling mechanisms shown in Figure 2(c) (i) and (ii): arm pulling is described by a contraction of the reference length ("negative growth") of the arms, while pushing off the ground is described by an increase in reference length ("growth") of the legs. Note that, while morphoelasticity is a theory of growth and remodelling [27], extensions of the theory have also been used to model muscle activation [28] or liquid crystal elastomer actuation [29]. In our case, the rods are taken to be rigid in flexion (no bending), but extensible. The lower body has reference length L_i^L and stiffness K_i^L (in unit force), and "growth" parameter γ_i^L, such that the reference length of the lower body under active body extension $\gamma_i^L \geq 1$ is $\gamma_i^L L_i^L$. Similarly, the arms have reference length[7] L_i^A, stiffness K_i^A, and activation parameter γ_i^A, such that the reference length of the arms under active arm pulling $\gamma_i^A \leq 1$ is $\gamma_i^A L_i^A$. The torso does not undergo any activation ($\gamma_i^T = 1$), and is moreover treated as an inextensible rod, that is, the lengths $\ell_i^T = L_i^T$ do not vary.

The third pulling mechanism we consider is a change in the stance of the players. To characterise this mechanism, we first need to outline a description of the external forces on each player, as depicted in Figure 2(b). Player 2 applies to Player 1 a force $-T\hat{\mathbf{e}}_r$, where T is the tension in the rope times its cross-sectional area, and

$$\hat{\mathbf{e}}_r := \frac{(x_1 - x_2)\hat{\mathbf{e}}_x + (y_1 - y_2)\hat{\mathbf{e}}_y}{\sqrt{(x_1 - x_2)^2 + (y_1 - y_2)^2}}$$

is the unit vector pointing from (x_2, y_2) to (x_1, y_1). By Newton's Third Law, the same force is applied in the opposite direction by Player 1 to Player 2. We assume that the rope is extensible with resting length R (distance measured between the hands of the two players) and spring constant k. For computational ease, we take each player's mass m_i to be concentrated at the centre of mass (only a small quantitative change would occur under a distributed mass description), thus giving a force $-m_i g\hat{\mathbf{e}}_y$ due to self-weight. The forces from the rope and gravity are balanced in equilibrium by a friction force F_i in the x-direction, and a vertical reaction force R_i in the y-direction, both acting at the point of contact between the body axis and the ground. We allow a rotation of the lower body about this point, and a separate rotation at the hips, both determined by balances of angular

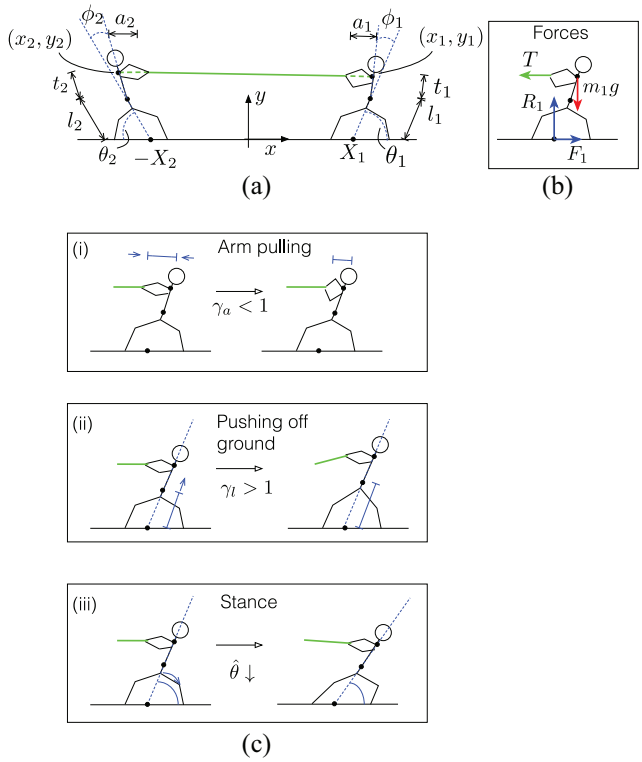

Figure 2. Schematic of our modelling framework. In (a), the variables defining the current configuration of each player are shown. The forces acting on each player (b) consist of a gravitational force due to self-weight, a force acting along the direction of the rope and equal in magnitude to the tension in the rope, and friction and reaction forces. In reality, there would be a set of friction and reaction forces at each foot, but we idealise these to a single set. In (c), the three mechanisms of activation for each player are shown: (i) arm pulling, in which the player shortens the arms, (ii) pushing off the ground, in which the lower body is extended, and (iii) a change in stance, defined by body orientation with respect to the horizontal.

momentum. To model the stance of the body as an active process, we define a reference angle $\hat{\theta}_i$, such that if the current angle of the body axis, θ_i, differs from the reference angle, a restoring torque $\kappa_i^L(\theta_i - \hat{\theta}_i)$ is produced. A change in stance can then be accounted for by decreasing the reference angle, as in Figure 2(c) (iii). A similar restoring torque $\kappa_i^T \phi_i$ is produced by bending at the hips.

In this mechanical description, the objective of each player is to make the other player either slip or stumble. Under dry friction, slipping will occur if $F_i/R_i > \mu_i$, where μ_i is the friction coefficient [30]. In general, μ_i will depend strongly on the surface on which the game is being played, as well as the footwear of each player. For a fair comparison, we suppose $\mu_1 = \mu_2$, and therefore our approach will be to analyse the relative values of F_i/R_i as we vary the other parameters in the system. Stumbling is a dynamic action, and so we defer its description to a later section.

3. Static analysis

We begin by considering a completely static game, in which both players are in mechanical equilibrium, and activation parameters $\{\gamma_i^L, \gamma_i^A, \hat{\theta}_i\}$ are varied slowly enough so that quasi-static equilibrium is maintained.

A force balance on Player 1 reads

$$-T\hat{\mathbf{e}}_r - m_1 g\hat{\mathbf{e}}_y + R_1\hat{\mathbf{e}}_y + F_1\hat{\mathbf{e}}_x = \mathbf{0}. \tag{1}$$

Balance of angular momentum for the lower body, about the point $(X_1, 0)$, takes the form

$$\ell_1^L(\cos\theta_1\hat{\mathbf{e}}_x + \sin\theta_1\hat{\mathbf{e}}_y) \times \left(T\hat{\mathbf{e}}_r + m_1 g\hat{\mathbf{e}}_y\right) = -\kappa_1^L(\theta_1 - \hat{\theta}_1)\hat{\mathbf{e}}_z. \tag{2}$$

Here, we have used the fact that forces applied to the upper body are directly transmitted through the torso to the lower body. For the upper body, the balance of angular momentum about the hips reads

$$L_1^T\left[\cos(\theta_1+\phi_1)\hat{\mathbf{e}}_x+\sin(\theta_1+\phi_1)\hat{\mathbf{e}}_y\right]\times\left(T\hat{\mathbf{e}}_r+m_1g\hat{\mathbf{e}}_y\right) = -\kappa_1^T\phi_1\hat{\mathbf{e}}_z. \tag{3}$$

Similar equations hold for Player 2, though noting sign changes due to the directionality of the rope, orientation angles being defined from the negative x-axis, and friction force pointing to the left:

$$T\hat{\mathbf{e}}_r-m_2g\hat{\mathbf{e}}_y+R_2\hat{\mathbf{e}}_y-F_2\hat{\mathbf{e}}_x=\mathbf{0}, \tag{4}$$

$$\ell_2^L(\cos\theta_2\hat{\mathbf{e}}_x-\sin\theta_2\hat{\mathbf{e}}_y)\times\left(T\hat{\mathbf{e}}_r-m_2g\hat{\mathbf{e}}_y\right) = \kappa_2^L(\theta_2-\hat{\theta}_2)\hat{\mathbf{e}}_z, \tag{5}$$

$$L_2^T\left[\cos(\theta_2+\phi_2)\hat{\mathbf{e}}_x-\sin(\theta_2+\phi_2)\hat{\mathbf{e}}_y\right]\times\left(T\hat{\mathbf{e}}_r-m_2g\hat{\mathbf{e}}_y\right) = \kappa_2^T\phi_2\hat{\mathbf{e}}_z. \tag{6}$$

Since the "arms" and lower body are not a fixed length, we also require a force balance plus constitutive description to determine the values of ℓ_i^A and ℓ_i^L. Following the notation by Moulton et al. [26], we define $\mathbf{n}_i = n_{x,i}\hat{\mathbf{e}}_x + n_{y,i}\hat{\mathbf{e}}_y$ to be the resultant force in the lower body. As we neglect bending of the body in this description, and all external forces are applied at the ends, we have

$$\mathbf{n_1} = -T\hat{\mathbf{e}}_r - m_1g\hat{\mathbf{e}}_y, \tag{7}$$

$$\mathbf{n_2} = T\hat{\mathbf{e}}_r - m_2g\hat{\mathbf{e}}_y. \tag{8}$$

The axial component of $\mathbf{n}_i$ is related to the elastic axial compression ratio $\alpha_i^L := \ell_i^L/\gamma_i^L L_i^L$ via a constitutive relation. Here, it is reasonable to assume small deformation, described by Hooke's law:

$$\mathbf{n_1}\cdot(\cos\theta_1\hat{\mathbf{e}}_x+\sin\theta_1\hat{\mathbf{e}}_y) = K_1^L(\alpha_1^L-1), \tag{9}$$

$$\mathbf{n_2}\cdot(-\cos\theta_2\hat{\mathbf{e}}_x+\sin\theta_2\hat{\mathbf{e}}_y) = K_2^L(\alpha_2^L-1). \tag{10}$$

Since the axis of the arms is assumed to lie along the line of the rope, the resultant force n_i^A in the arms is equal to the tension in the rope, that is

$$n_1^A = n_2^A = T, \tag{11}$$

and we assume again a linear constitutive relation between force and extension,

$$n_1^A = K_1^A\left(\frac{\ell_1^A}{\gamma_1^A L_1^A}-1\right), \tag{12}$$

$$n_2^A = K_2^A\left(\frac{\ell_2^A}{\gamma_2^A L_2^A}-1\right). \tag{13}$$

The rope also satisfies Hooke's law:

$$T = k(r-R), \tag{14}$$

where $r = \left[(x_1-x_2)^2+(y_1-y_2)^2\right]^{1/2} - (\ell_1^A+\ell_2^A)$ is the current rope length between the two grip points. The spring constant $k = EA/R$, where E is the Young's modulus for the rope, A is the cross-sectional area, and as noted R is the rest length. Here, we use a value $k = 5\times10^4$ N/m, corresponding to a material with $E\sim10$ GPa, $A\sim10$ mm^2, and $R\sim2$ m.

Note also the geometric relations

$$x_1 = X_1+\ell_1^L\cos\theta_1+L_1^T\cos(\theta_1+\phi_1), \tag{15}$$

$$y_1 = \ell_1^L\sin\theta_1+L_1^T\sin(\theta_1+\phi_1), \tag{16}$$

$$x_2 = -X_2-\ell_2^L\cos\theta_2-L_2^T\cos(\theta_2+\phi_2), \tag{17}$$

$$y_2 = \ell_2^L\sin\theta_2+L_2^T\sin(\theta_2+\phi_2). \tag{18}$$

From the above, we obtain a closed system as follows. Considering Player 1, we insert the force balance (7) into the body constitutive law (9), and the arms force balance (11) into the constitutive law (12). These two equations are combined with the moment balances (2) and (3) for the lower and upper body, respectively. Doing the same for Player 2 leads to a set of eight equations. Noting that the rope tension T is a function of the body lengths $\{\ell_1^L, \ell_2^L\}$, arm lengths $\{\ell_1^A, \ell_2^A\}$, and body angles $\{\theta_1, \theta_2, \phi_1, \phi_2\}$ via the constitutive relation (14) and geometric relations (15)–(18), the system is fully determined by the eight variables $\mathcal{S} := \{\ell_1^L, \ell_2^L, \ell_1^A, \ell_2^A, \theta_1, \theta_2, \phi_1, \phi_2\}$. Therefore, given material and geometric parameters

$$\begin{aligned}\mathcal{M} := \{&K_1^L, K_2^L, K_1^A, K_2^A, m_1, m_2, \kappa_1^L, \kappa_2^L,\\ &k, R, L_1^L, L_2^L, L_1^T, L_2^T, L_1^A, L_2^A, X_1, X_2\}\end{aligned} \tag{19}$$

and activation parameters $\mathcal{A} := \{\gamma_1^L, \gamma_2^L, \gamma_1^A, \gamma_2^A, \hat{\theta}_1, \hat{\theta}_2\}$ we have eight equations to solve for the eight variables $\mathcal{S}$. Then, given a solution, we can check for slipping by computing the friction F_i and reaction R_i components from equations (1) and (4), asking whether the slipping criterion $F_i/R_i > \mu_i$ is met for either player.

3.1. Mass is (almost) everything

Before considering specific solutions to the static system, we demonstrate the challenge of beating a heavier opponent in a static game. This comes as a simple consequence of the form of the friction and reaction components. Namely, equation (1) gives

$$\frac{F_1}{R_1} = \frac{T\hat{\mathbf{e}}_r \cdot \hat{\mathbf{e}}_x}{m_1 g + T\hat{\mathbf{e}}_r \cdot \hat{\mathbf{e}}_y}, \tag{20}$$

while equation (4) gives

$$\frac{F_2}{R_2} = \frac{T\hat{\mathbf{e}}_r \cdot \hat{\mathbf{e}}_x}{m_2 g - T\hat{\mathbf{e}}_r \cdot \hat{\mathbf{e}}_y}. \tag{21}$$

Since the rope pulls equally on both players, and the friction forces point in opposite directions, the friction components are the same. Naturally, the reaction components each include a component balancing the weight, so that if the rope is horizontal, that is, $\hat{\mathbf{e}}_r \cdot \hat{\mathbf{e}}_y = 0$, the reaction force will be higher for the player with more mass, and they will have the advantage. In a typical game, the rope tends to be sufficiently long so that $\hat{\mathbf{e}}_r \cdot \hat{\mathbf{e}}_y$ is negligible. Under the approximation $\hat{\mathbf{e}}_r \cdot \hat{\mathbf{e}}_y \ll 1$, and supposing that $m_1 > m_2$, victory is hopeless for the lighter Player 2: No matter what activation they apply, we will have $F_1 \approx F_2$ and $R_1 > R_2$, so that they will always slip before their opponent. Nevertheless, for $\hat{\mathbf{e}}_r \cdot \hat{\mathbf{e}}_y$ sufficiently large, it is not entirely hopeless, and comparing the slipping criteria above suggests the only possible strategy for the lighter player, which consists of getting higher than their opponent [24]. With $m_1 > m_2$, if Player 2 can get higher than Player 1, that is. $y_2 > y_1$, then $\hat{\mathbf{e}}_r \cdot \hat{\mathbf{e}}_y < 0$, so that the rope pulls Player 2 down, increasing their reaction force, while pulling Player 1 up and decreasing their reaction force. However, this strategy is possible only if the rope is sufficiently short, which does not correspond to a realistic scenario (typically $R \approx 10$ m, see [9]).

3.2. Parameters

To analyse in detail the effect of the different types of activation, we first fix baseline material and geometric parameters, listed in Table 1. A discussion of these parameter choices is provided in Appendix 1.

3.3. Static activation

Figure 3 shows the results of a simulated 'static' game in which Player 1 (blue) has a slight advantage in mass, with $m_1 = 41$ kg and $m_2 = 40$ kg, and all other parameters taken to be equal. We then simulate independently each of the three pulling mechanisms for Player 2 and plot the resulting slipping components F_i/R_i and rope tension T. The configurations of the players at the indicated positions are shown in the insets, where the dashed lines denote the reference states.

In Figure 3(a), we consider arm activation for Player 2, $\gamma_2^A < 1$. As arm activation increases (γ_2^A decreases), the tension in the rope increases, and F_i/R_i increases for both players. However, Player 2 begins at a disadvantage, that is, $F_2/R_2 > F_1/R_1$ before the activation, and the increasing tension means that the difference

Table 1. Material and geometric parameters.

Parameter	Description	Value
K_i^L	Lower body stiffness	3000 N
K_i^A	Arm stiffness	500 N
κ_i^L	Stance rotational stiffness	1000 N
m_i	(Concentrated) body mass	40 kg
X_i	Players' distance from origin	2 m
L_i^L	Lower body length (to hips)	0.8 m
$\ell_i^T = L_i^T$	Upper body length (to concentrated mass)	0.5 m
L_i^A	Rest arm length (torso to hold point)	0.5 m
k	Rope spring constant	5×10^4 N/m
R	Rope resting length	3.4 m
$\mathcal{I}_i^L$	Lower body moment of inertia	5 kg m^2
ζ_i^L	Lower body rotational drag coefficient	150 N m s
$\mathcal{I}_i^T$	Upper body moment of inertia	5 kg m^2
ζ_i^T	Upper body rotational drag coefficient	150 N m s
m_i^A	Arms mass	4 kg
ζ_i^A	Arms drag coefficient	50 kg/s
ζ_i^T	Body drag coefficient	100 kg/s

$F_2/R_2 - F_1/R_1$ actually increases slightly with increasing arm activation; that is, Player 2 has only made their situation worse.

Figure 3(b) shows the result of leg activation for Player 2, that is, $\gamma_2^L > 1$. Again, the tension increases, though by a smaller amount. In this case, leg activation increases the height of Player 2, which as noted above is advantageous (albeit not dramatically). We see that $F_2/R_2 - F_1/R_1$ decreases with increasing γ_2^L, and Player 2 even gets the advantage for $\gamma_2^L \gtrsim 1.8$ (though this corresponds to a 180% extensional increase, which is only possible if the player begins in a significantly crouched state, which in practice constitutes a foul, see [9]).

Figure 3(c) considers a change in the stance of Player 2, in particular a decrease in $\hat{\theta}_2$ from the original base value of 1.2, meaning that Player 2 is trying to lean further backwards as $\hat{\theta}_2$ decreases. The situation is similar to arm activation: leaning back increases the tension, but because Player 2 begins at a disadvantage, this only serves to increase their disadvantage, $F_2/R_2 - F_1/R_1$ increases with decreasing $\hat{\theta}_2$. Observe that the tension reaches the highest value in this simulation, and therefore so also does the F_i/R_i, demonstrating that a change in stance was the worst choice for Player 2 of these activation strategies. If $\mu = 0.8$, for instance, then Player 2 will have caused themselves to slip.

4. Dynamics

Having established the severe disadvantage of a lighter player in a quasistatic equilibrium, in this section, we turn to dynamics. In particular, we focus on two types of dynamic motion: a sudden pulling of the rope, and a sudden change in stance. Mathematically, these correspond to taking γ_i^A and $\hat{\theta}_i$ to be functions of time t, with a fast-enough rate of change that inertial effects are not negligible.

From these dynamic activations, we consider slipping in a dynamic sense, defined in the same way as the static case, as the ratio F_i/R_i exceeding the friction coefficient μ. Along with slipping, in a dynamic setting, we also consider stumbling, which corresponds to a rapid acceleration forward of the torso, sufficient to cause the player to momentarily lose balance and have to take a step forward. This will be defined mathematically below, but note that, intuitively, these are distinct, and getting the opponent to slip and/or stumble is the key to winning a game of tug of war.

For computational simplicity, in this section, we fix the lower body length, and include inertial terms in the balances of linear and angular momentum. The momentum balance for the lower body of Player 1 is

$$\begin{aligned}\mathcal{I}_1^L\ddot{\theta}_1 + \zeta_1^L\dot{\theta}_1 &= -\kappa_1^L(\theta_1 - \hat{\theta}_1)\hat{\mathbf{e}}_z \\ &+ \ell_1^L(\cos\theta_1\hat{\mathbf{e}}_x + \sin\theta_1\hat{\mathbf{e}}_y) \times \left(-T\hat{\mathbf{e}}_r - m_1 g\hat{\mathbf{e}}_y\right).\end{aligned} \tag{22}$$

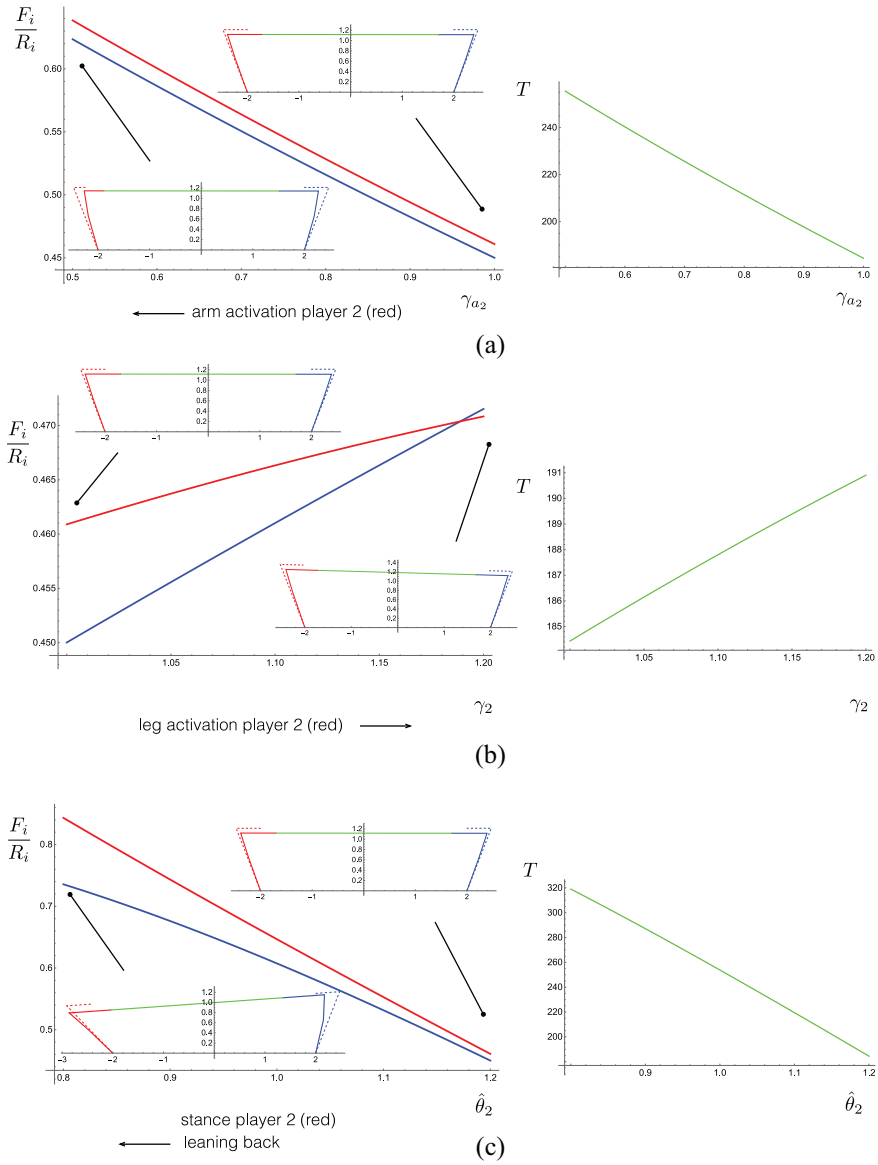

Figure 3. Simulation of a quasistatic game. Player 2 employs arm activation (a), leg activation (b), and a change in stance (c). The friction ratios F_i/R_i are plotted at left in each case for both Player 1 (blue) and Player 1 (red). The configuration of the system is shown as insets at the indicated points, with solid lines showing the position of the lower body, upper body, and arms, while dashed lines show the respective reference states. At right, the tension in the rope is plotted against the activation parameter.

Here, the right-hand side contains the same torque terms as the static moment balance (2). The left-hand side includes the rate of change of angular momentum about the pivot point $(X_1, 0)$, with moment of inertia $\mathcal{I}_1^L$, and overdots denoting time derivatives; we also include a damping term ζ_1^L to suppress oscillations. The moment balance for the upper body of Player 1 reads

$$\begin{aligned}\mathcal{I}_1^T\ddot{\phi}_1 + \zeta_1^T\dot{\phi}_1 &= -\kappa_1^T\phi_1\hat{\mathbf{e}}_z \\ &- L_1^T\left[\cos(\theta_1+\phi_1)\hat{\mathbf{e}}_x + \sin(\theta_1+\phi_1)\hat{\mathbf{e}}_y\right] \times \left(T\hat{\mathbf{e}}_r + m_1 g\hat{\mathbf{e}}_y\right).\end{aligned} \tag{23}$$

Similarly, the moment balances for Player 2 are

$$\begin{aligned}\mathcal{I}_2^L\ddot{\theta}_2 + \zeta_2^L\dot{\theta}_2 &= -\kappa_2^L(\theta_2 - \hat{\theta}_2)\hat{\mathbf{e}}_z \\ &+ \ell_2^L(\cos\theta_2\hat{\mathbf{e}}_x - \sin\theta_2\hat{\mathbf{e}}_y) \times \left(T\hat{\mathbf{e}}_r - m_2 g\hat{\mathbf{e}}_y\right),\end{aligned} \tag{24}$$

and

$$\mathcal{I}_2^T\ddot{\phi}_2 + \zeta_2^T\dot{\phi}_2 = -\kappa_2^T\phi_2\hat{\mathbf{e}}_z + L_2^T\left[\cos(\theta_2+\phi_2)\hat{\mathbf{e}}_x - \sin(\theta_2+\phi_2)\hat{\mathbf{e}}_y\right]\times\left(T\hat{\mathbf{e}}_r - m_2g\hat{\mathbf{e}}_y\right). \tag{25}$$

Along with these, we require an inertial force balance for the arms. This takes the same form for both players:

$$m_i^A\ddot{\ell}_i^A + \zeta_i^A\dot{\ell}_i^A = T - K_i^A\left(\frac{\ell_i^A}{\gamma_i^A L_i^A} - 1\right). \tag{26}$$

Again the right-hand side includes the static force balance, while the left-hand side includes an acceleration term, with m_i^A the mass of the arms, and a damping term with coefficient ζ_i^A.

Taking the torso and leg lengths ℓ_i^T and ℓ_i^L to be fixed in a dynamic setting and noting again that the tension is given by the geometric relations (15)–(18) and the constitutive relation (14), for given material and activation parameters, the dynamic system is fully defined by the variables $\mathcal{S}_{\text{dyn}} = \{\theta_1(t), \theta_2(t), \phi_1(t), \phi_2(t), \ell_1^A(t), \ell_2^A(t)\}$, which are found by integrating the six differential equations above. Having solved for $\mathcal{S}_{\text{dyn}}$, we can then evaluate whether slipping would have occurred during the dynamic motion by considering the dynamic force balance equations. For Player 1, this is given by

$$m_1(\ddot{x}_1\hat{\mathbf{e}}_x + \ddot{y}_1\hat{\mathbf{e}}_y) + \zeta_1(\dot{x}_1\hat{\mathbf{e}}_x + \dot{y}_1\hat{\mathbf{e}}_y) = -T\hat{\mathbf{e}}_r - m_1g\hat{\mathbf{e}}_y + R_1\hat{\mathbf{e}}_y + F_1\hat{\mathbf{e}}_x, \tag{27}$$

while for Player 2 this reads

$$m_2(\ddot{x}_2\hat{\mathbf{e}}_x + \ddot{y}_2\hat{\mathbf{e}}_y) + \zeta_2(\dot{x}_2\hat{\mathbf{e}}_x + \dot{y}_2\hat{\mathbf{e}}_y) = T\hat{\mathbf{e}}_r - m_2g\hat{\mathbf{e}}_y + R_2\hat{\mathbf{e}}_y - F_2\hat{\mathbf{e}}_x. \tag{28}$$

Since the terms $(x_1(t), y_1(t))$, $(x_2(t), y_2(t))$, and $T(t)$ are all given in terms of $\mathcal{S}_{\text{dyn}}$, equations (27) and (28) can be solved for $(F_1(t), R_1(t))$ and $(F_2(t), R_2(t))$, and the slipping criterion $F_i/R_i > \mu$ may thus be evaluated dynamically (noting that for given μ, if at any time either of $F_i/R_i > \mu$, the motion ceases to be valid beyond that point, as that player will have slipped). Stumbling is a bit harder to quantify, as it is strongly dependent on catching the opponent off guard. We will equate a player losing balance and stumbling with the rotational acceleration of the torso exceeding a threshold, that is, $\ddot{\phi}_i > s^*$, where the threshold s^* could be determined either experimentally or through more detailed biomechanical modelling; but for our purposes, we will just explore the idea of stumbling qualitatively. In the analysis below, we again suppose that Player 1 has a slight mass advantage, $m_1 = 41\,\text{kg} > m_2 = 40\,\text{kg}$. We then analyse various strategies of Player 2, asking under what conditions Player 2 can make Player 1 slip or stumble, without Player 2 first slipping or stumbling.

4.1. Letting up

We first consider a strategy for causing Player 1 to slip. It is instructive to note from equation (27) that the dynamic friction force satisfies

$$F_1 = T\hat{\mathbf{e}}_r\cdot\hat{\mathbf{e}}_x + m_1\ddot{x}_1 + \zeta_1^L\dot{x}_1. \tag{29}$$

If Player 2 were to cause Player 1 to rapidly accelerate to the left, for example, by a sudden pulling of the rope, the immediate reaction would be a negative acceleration, that is, $\ddot{x}_1 < 0$. However, this would only serve to decrease the friction force of Player 1. At the same time, since

$$F_2 = T\hat{\mathbf{e}}_r\cdot\hat{\mathbf{e}}_x - m_2\ddot{x}_2 - \zeta_2^L\dot{x}_2, \tag{30}$$

the corresponding motion of both players to the left would also imply $\ddot{x}_2 < 0$, thereby *increasing* the friction force of Player 2. Therefore, by a sudden pulling, Player 2 cannot cause Player 1 to slip but can only cause themselves to slip. By the same logic, though, if Player 2 can cause the system to suddenly shift to the right, then $\ddot{x}_i > 0$, and the friction force of Player 1 (2) will go up (down), and Player 1 may slip. Player 2 could accomplish this strategy by suddenly "letting up" in a controlled way.

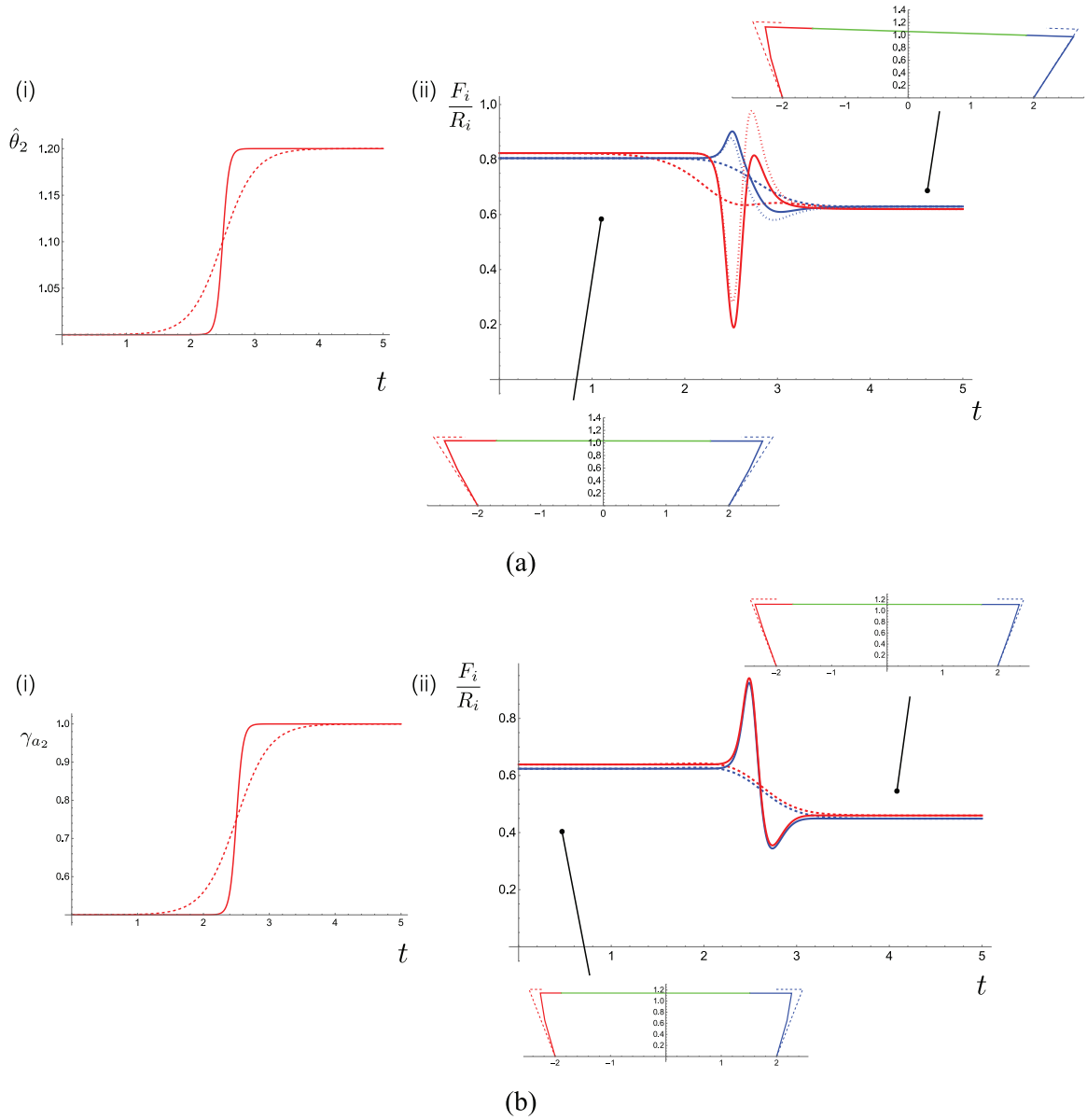

Figure 4. Dynamic simulations with Player 2 employing the "letting up" strategy. In (a), Player 2 makes their stance more vertical, by increasing $\hat{\theta}_2$; in (b), they lengthen their arms by increasing γ_2^A. The activation parameters are plotted against time in (i), in which we have simulated both a rapid (solid curves) and slower (dashed curves) change. In (ii), the corresponding friction ratios F_i/R_i are plotted, plus the configuration of the system before and after the change, with solid lines showing the position of the lower body, upper body, and arms, while dashed lines show the respective reference states. Parameter values are given in Table 1, but with $m_1 = 41$ kg; also the dotted curve in (a) (ii) is generated with $\zeta_1 = \zeta_2$ decreased to 10.

Figure 4 shows a simulation of Player 2 'letting up' in two different ways. In Figure 4(a) Player 2 shifts their stance to be more vertical, by increasing $\hat{\theta}_2$. Figure 4(a) (i) plots $\hat{\theta}_2$ as a function of time, where the simulation runs for $t = 5$ s. We consider two different rates of change, a slow change of stance (dashed curve), and a rapid change of stance (solid curve). Figure 4(a) (ii) plots the resulting slip ratios F_i/R_i as functions of time for Player 1 (blue) and Player 2 (red). Considering the flat portions of the curve, we see that in a static sense, Player 2's change of stance has served to decrease the slip ratio for both players, as their more vertical orientation decreases the rope tension, and in a static sense, the change of height has given Player 2 a slight advantage. With the slow change of stance, the slight acceleration to the right causes the curves to cross over during the

dynamic transition: for $1.5 \lesssim t \lesssim 3.5$, $F_1/R_1 > F_2/R_2$; however, this will not do Player 2 any good, as Player 1 never has a slip ratio higher than that with which Player started the motion.

On the contrary, in the case of the rapid change in stance, not only do the curves cross over, but the rapid acceleration to the left causes Player 1 to experience a momentary spike in slip ratio, reaching a peak of $F_1/R_1 \approx 0.9$ that exceeds the value Player 2 started with. If $\mu = 0.9$, this will have been a successful strategy in causing Player 1 to slip. However, this is a potentially dangerous strategy. The dotted curve shows the slip ratios for the same simulation but with a lower drag coefficient. While Player 1 again experiences a spike in slip ratio, the deceleration at the end of the motion causes Player 2 to experience an even higher spike. Thus, if Player 2 does not cause Player 1 to slip with the initial acceleration, they may cause themselves to slip with the subsequent deceleration.

In Figure 4(b), we simulate the same strategy of Player 2 letting up, but in this case, with their arms through an increase in γ_2^A. The time profile of γ_2^A is plotted on the left, and the corresponding slip ratios are plotted on the right. Again, we simulate both a slow release of the arms (dashed curve) and a rapid release (solid curves). Although the conceptual idea is the same, and the change in position has a similar static effect of decreasing the tension and slip ratio for both players, dynamically we observe a much different picture. With a slow change of stance, both players simply see a smooth decrease in slip ratio, and F_2/R_2 is always higher than F_1/R_1. In the case of a more rapid release, Players 1 and 2 experience simultaneous spikes and then dips in slip ratio and again with F_2/R_2 always slightly higher than F_1/R_1. The reason for this simultaneity can be understood by considering the static change in stance: both players end up with a less bent torso, that is, the motion is outward for both players, and the simultaneous acceleration away from each other causes an increase in friction force for each player. This is ultimately a bad strategy for Player 2: if the spike in F_i/R_i is enough to cause slipping, they will slip a moment before. Interestingly, the proximity of the curves could result in both players slipping simultaneously, though it is beyond the scope of this work to examine post-slipping dynamics.

4.2. Quick pull

In Figure 5, we analyse an alternative dynamic strategy of a rapid pulling of the rope in an attempt to make the opponent stumble. As in Figure 4(b), a quick pull with the arms has a symmetric effect, that is, both players move towards each other, and Player 2 cannot gain an advantage over Player 1. Therefore, with all other parameters equal, we restrict our analysis to rapid pulling via a change in stance by decreasing $\hat{\theta}_2$. Figure 5(a) (i) plots $\hat{\theta}_2$ as a function of time, where again we simulate both a slow change in stance (dashed curve) and a rapid change in stance (solid curve). In Figure 5(a) (ii), we plot the rotational acceleration of the torso, $\ddot{\phi}_i$ during the motion, for both Player 1 (blue) and Player 2 (red). For both the slow and rapid change, the shift of the system to the left causes an acceleration and subsequent deceleration of Player 1's torso, as they are pulled forward. In the case of the rapid change in stance, since Player 2 has changed the stance of their lower body, their upper body actually experiences an initial forward acceleration as well, though significantly smaller than Player 1's. The large spike in $\ddot{\phi}_1$ may be sufficient to cause Player 1 to stumble. However, this is again a potentially dangerous strategy. Figure 5(a) (iii) plots the slip ratios through the dynamic motion, showing that the rapid movement to the left creates a large spike in F_2/R_2. Whether Player 2 can cause Player 1 to stumble without first causing themselves to slip will be strongly dependent on the specifics of the surface and preparedness of Player 1.

Thus far, we have simulated players with identical properties aside from the slight mass advantage of Player 1. Of course, in reality, players will likely differ across a spectrum of characteristics, both in strength and size. As a final example, we simulate in Figure 5(b) a rapid arm pull by Player 2, still with the same mass disadvantage, but with a significantly stronger upper body, by taking $K_2^A = 5K_1^A$ (arm stiffness), and $\kappa_2^T = 2\kappa_1^T$ (rotational stiffness of the torso, modelling increased core and abdominal strength). Figure 5(b) (i) plots the arm activation $\gamma_2^A(t)$, while Figure 5(b) (ii) and (iii) plot the rotational acceleration and slip ratios during the motion. For comparison, in the insets of Figure 5(b) (ii) and (iii), we plot the results under equal upper body strength. Perhaps surprisingly, even with the significant advantage in upper body strength, the arm pull does not give Player 2 much, if any, advantage. The shortening of Player 2's arms causes both players' torsos to accelerate and then decelerate forward; simultaneously they each experience a dip and then spike in frictional force. With equal upper body strength, the rotational accelerations are nearly identical while Player 2 has a slightly higher slip ratio. In the case of Player 2 having increased upper body strength, Player 1 experiences a higher rotational acceleration, though only slightly, but still the less-massive Player 2 has a higher slip ratio. It seems, for these parameters, that the rapid arm pull is not a good strategy for Player 2.

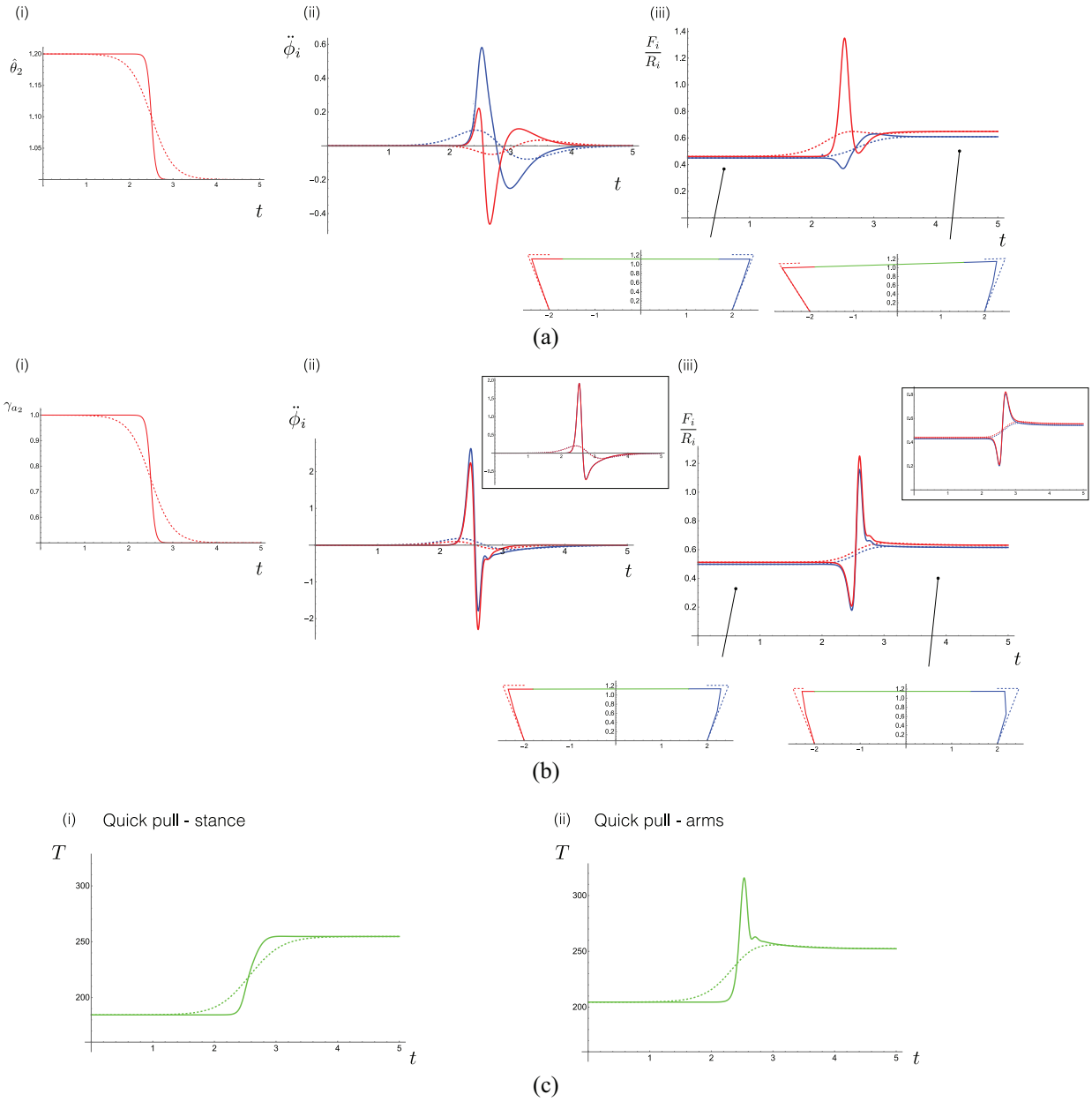

Figure 5. Dynamic simulations with Player 2 employing the "Quick pull" strategy. In (a), Player 2 makes their stance less vertical, in (b) they shorten the arms. Profiles of $\hat{\theta}_2$ and γ_2^A plotted against time in (a) (i) and (b) (i), each simulated both with rapid change (solid curve) and less rapid change (dashed curve). In (a) (ii) and (b) (ii), the potential for stumbling is shown by plotting the rotational acceleration of the upper body, $\ddot{\phi}_i$. In (a) (iii) and (b) (iii), the slip ratio F_i/R_i is shown dynamically, and the configuration of the system is shown before and after the dynamic motion, with solid lines showing the position of the lower body, upper body, and arms, while dashed lines show the respective reference states. In (c), the tension in the rope is plotted dynamically for the simulations of (a) and (b) (the unequal body strength case). Parameter values are given in Table 1, but with $m_1 = 41$ kg, and with K_2^A increased to 2500 and κ_2^T increased to 800 in (b) (ii) and (b) (iii) main plots.

As mentioned in the introduction, one predominant cause of injuries/casualties is the extremely fast release of energy that occurs in the event of rope failure. This will happen if the tension in the rope exceeds a critical threshold. Here, it is important to note that the tension is also a dynamic variable, and a static analysis of the potential forces applied by players is insufficient. To demonstrate, in Figure 5(c) we plot the tension in the rope corresponding to the rapid pulls from Figure 5(a) and (b). In the case of the change in stance, Figure 5(c) (i), even with a rapid change in stance, the tension transitions between the static values smoothly and nearly

monotonically. However, with the arm pull, and with the significant upper body strength of Player 2, Figure 5(c)(ii), there is a large spike in the tension during the dynamic motion, reaching a maximum value that is 25% higher than the final static value.

5. Discussion

Mathematical modelling of sport is inherently challenging. Biomechanical and/or physiological descriptions of a specific motion of the body during sport are already complex and high-dimensional, potentially involving the activation of numerous muscle groups, tendon mechanics, joint reaction forces, heart rate, oxygen uptake, neuromechanical effects, energy expenditure, stamina, among other processes [31–34]. Naturally, the complexity only increases when including variable motion, multiple people physically interacting, detailed tactics, and intangible factors such as psychological momentum [35]. Of course, these complexities are part of what makes the outcome of a sporting event unpredictable and perhaps ultimately what makes sport entertaining. In terms of modelling, though, it is clear that a detailed mathematical description of any sport would likely be completely intractable. Sports predictions, for example, for betting purposes, are usually based on play-by-play simulation, for example, with Markov Chain decisions, or direct simulation [36, 37], both of which are data-driven approaches that rely on statistics from previous results and do not explicitly include any mechanics. Nevertheless, most sports are intrinsically mechanical, and training largely involves preparing the body to complete a mechanical task in a near-optimal way.

In this paper, we have developed and analysed a mathematical model of the mechanics of a game of tug of war between two players. In light of the complexities outlined above, tug of war provides perhaps an ideal case study for investigating mechanics in sport. At a glance, the game appears simple: two teams pull on opposite ends of a rope, and whichever team pulls harder will win. However, a closer look quickly reveals a number of complexities in the game, characterised by multiple degrees of freedom, non-trivial mechanics, and various strategic choices open to the players. Still, the game is largely played in approximate mechanical equilibrium, and physical motions are relatively simple; this combination means that an idealised mathematical description is possible in which governing equations remain solvable while still containing sufficient detail and degrees of freedom to explore the intricacies of the game. While previous papers have exploited this relative simplicity to derive mechanical descriptions of rope pulling, our analysis provides the first mechanical description capable of simulating an actual game, in which player strategy may be explicitly investigated.

Beginning with an analysis of a static game, we first showed that a lighter player is at a significant disadvantage. While this observation is not new [25], our analysis provides in simple equation form the challenge faced by the lighter player, and our quantitative analysis illustrated the possibility of gaining the advantage by becoming taller through leg activation as well as how some forms of pulling activation, in fact, make the situation worse. We then turned to a dynamic description of the game, and focused on the simple questions: *Can the lighter player win?*, and if so, *what is their best strategy?* In our modelling framework, a strategy consists of a time-dependent change in one or more of the reference properties of the player which would, in a more detailed biomechanical description, be mapped to contraction of the relevant muscle groups. It is important to highlight here the distinction between the reference lengths and the actual lengths. For instance, in an "arm pull" strategy, the player activates their arm muscles in an attempt to bring their hands closer to their torso. But this does not mean that they will necessarily shorten the arm length; it is only in solving the force and moment balances, that is, considering all the variables, that one can determine how much they actually change the state of the system.

In quantifying the success of a strategy, we have made the important distinction between stumbling, in which the player's upper body is suddenly pulled forward causing a loss of balance, and slipping, in which the ratio of friction force to reaction force at the feet exceeds the slipping threshold. The former is induced by an acceleration of the upper body towards the other player, while the latter is, somewhat counter-intuitively, induced by the opposite, an acceleration away from the other player. By simulating sudden changes in activation by the lighter player, we demonstrated that inertial activations do exist for which the lighter player can cause the heavier player to slip or stumble but that the success is highly dependent on the activation rate. This analysis also highlighted the dual nature of any activation: in each case, the execution by the lighter player must be just right in order to avoid causing themselves to first slip or stumble.

While our analysis has focused on the possibility of a lighter player beating a heavier player, there are many more directions of analysis within our modelling framework that could be interesting, for instance, if the players have equal mass but differing strength characteristics (modelled e.g. by unequal stiffness parameters), how does such asymmetry impact the dynamics of the game? The strategies that can be investigated with our

model are in principle straightforward to implement in a real game. Whether these would result in outcomes in line with model predictions depends on a number of factors, and suggests some useful directions for future research. Qualitative features are likely to hold, as these are consequences of the basic physics underlying the game. A strong quantitative agreement is unlikely given the idealisations built into the model, though this may be possible if the mechanical stiffness parameters were tuned. We have made efforts to determine realistic parameters, which in the case of mechanical stiffness values has required its own separate modelling, with assumptions and idealisations therein. More realistic values may be attainable with more detailed modelling, and/or the values could be calibrated to a player and/or game. A particularly useful direction for future research would be to link biomechanical descriptions of muscle contractions with the idealised activation parameters $\mathcal{A} := \{\gamma_1^L, \gamma_2^L, \gamma_1^A, \gamma_2^A, \hat{\theta}_1, \hat{\theta}_2\}$ in our model. This would provide a means of constraining the range of input values for $\mathcal{A}$ in terms of specific muscle capabilities and thus would enable to more explicitly assess the feasibility of implementing a given strategy.

To the best of our knowledge, this paper provides the first attempt to analyse tug of war mechanically, from the angle of the competition between several players, in contrast to biomechanical approaches that focus on the pulling performances of one player. For the sake of simplicity, we restricted our attention to the case of two opponents, while evidently, actual tugging war contests involve more players; from eight players per team as per the Tug of War International Federation standards [9], up to several hundred on much rarer occasions. The team strategy and collective dynamics that emerge from a large number of players may be non-intuitive and include potentially interesting aspects of nonlinear complex systems and collective behaviours, such as synchronisation, waves, spontaneous oscillations, or resonance-like effects.

Overall, our relatively simple modelling strategy has captured essential features of the game and illustrated somewhat non-intuitive strategic consequences, emerging from basic Newtonian mechanics. To make progress, our approach should be combined with recent advances in computational human biomechanics to improve our analysis of the complex winning ways of the oldest game in humanity.

> "The only thing that truly matters in what we do is having fun."
>
> Alain Goriely

Acknowledgements

The authors extend their warmest congratulations to their colleague Alain Goriely for his election as Fellow of the Royal Society of London. His approach and contributions to science and mathematics are inspiring, and the authors are sincerely grateful for his unwavering, friendly support, invaluable trust, and significant intellectual influence. This work was performed in secrecy. It is thus with a subtle nod that HO attributes the covert triumph of this mischievous plot to Alain's distinctive aversion to micro-management. The authors are also grateful to Chad G. Petri, whose enigmatic yet invaluable conversations about tug of war and almost algorithmic writing precision contributed to the finalisation of the introduction.

Declaration of conflicting interests

Mathematical notebooks with implementation of the model and output of model results are available upon request.

Funding

The author(s) received no financial support for the research, authorship, and/or publication of this article.

ORCID iDs

Derek E Moulton https://orcid.org/0000-0003-3597-7973

Hadrien Oliveri https://orcid.org/0000-0002-5488-5567

Notes

1. A ropeless version of tug of war is depicted in the tomb of Mereruka (Saqqara, Egypt, ca. 2000 BC). Here two players hold hands and are pulled by their respective teams from behind.

2. A tug of war between *asuras* and *devas*, as part of the Hindu myth of Samudra Manthana, is shown on a stone relief in Angkor Wat (12th century).
3. The Sun Temple of Konark (13th century) has a stone relief showing a game of tug of war.
4. The Nation (October 27, 1997), *Two lose arms in Taiwan tug-of-war*.
5. AP News (June 6, 1995), *Two Boy Scouts Killed In Tug-of-War Accident*.
6. Priceconomics (March 8, 2017), *A History of Tug-of-War Fatalities*.
7. The reference length here is not the length of the arms but the distance between the holding point with the rope and the torso when the arm muscles are not contracted.

References

[1] Tug. Oxford English Dictionary, https://www.oed.com/view/Entry/207293?redirectedFrom=tug+of+war#eid17441785
[2] Park, W (ed.). *Tugging rituals and games a common element, diverse approaches (Living heritage series)*. Jeonju, South Korea: ICHCAP, 2019.
[3] Cayero, R, Rocandio, V, Zubillaga, A, et al. Analysis of tug of war competition: a narrative complete review. *Int J Environ Res Public Health* 2021; 19(1): 3.
[4] Li, X. The origin, development and winning skills of tug of war. *Open Cybern Syst J* 2015; 9(1): 2021–2024.
[5] Houdin, JP, and Houdin, H. La construction de la pyramide de Khéops: vers la fin des mystères? *Ann Ponts Chauss* 2002; 2002(101): 76–84.
[6] Andreu-Cabrera, E, González, MC, Ruis, FJR, et al. Play and childhood in ancient Greece. *J Hum Sport Exerc* 2010; 5(3): 339–347.
[7] Eichberg, H. Three dimensions of pull and tug: towards a philosophy of popular games. *Stud Phys Cult Tour* 2003; 10(1): 51–73.
[8] Perkins, R. *Thor the Wind-raiser and the Eyrarland image*. London: Viking Society for Northern Research, 2001.
[9] Tug of War International Federation (TWIF). TWIF rules manual, 2023, https://tugofwar-twif.org/2016/08/05/rules/
[10] Williams, S. *The boy's treasury of sports, pastimes, and recreations*. 4th ed. New York: Clark, Austin & Smith Publisher, 1854.
[11] Routledge, E (ed.). *Every boy's book: a complete encyclopædia of sports and amusements*. 2nd ed. London and New York: George Routledge & Sons, 1869.
[12] McMillen, T, and Goriely, A. Tendril perversion in intrinsically curved rods. *J Nonlinear Sci* 2002; 12(3): 241–281.
[13] Tutar, H. Can Squid Game series be watched through social darwinism? A semiotic review. *Turk Rev Commun Stud* 2022; 41: 1–22.
[14] Campillo, DA, Espinoza, JJV, Bahamón, MJR, et al. Reflexiones filosóficas sobre el juego del Calamar-Squid Game serie de Netflix. *Revista Filos* 2021; 38(99): 304–315.
[15] Chotai, PN, and Abdelgawad, AA. Tug-of-war injuries: a case report and review of the literature. *Case Rep Orthop* 2014; 2014: 519819.
[16] Smith, J, and Krabak, B. Tug of war: introduction to the sport and an epidemiological injury study among elite pullers. *Scand J Med Sci Sports* 2002; 12(2): 117–124.
[17] Pawlowski, RF, Palumbo, FC, and Callahan, JJ. Irreducible posterolateral elbow dislocation: report of a rare case. *J Trauma Acute Care Surg* 1970; 10(3): 260–266.
[18] Yamamoto, H, Kawahara, S, and Wakayama, H. A biomechanical analysis on tug of war. *Stud Educ Technol* 1988; 14: 127–132.
[19] Liou, C, Wong, TL, Wang, JC, et al. The study of team resultant force vanishing percentage in elite tug of war players. In: *Proceedings of the 23th international symposium on biomechanics in sports*, Beijing, China, 22–27 August 2005.
[20] Tanaka, K, Kawahara, S, Minamitani, N, et al. Analysis of timing skill of drop exercise in elite indoor tug of war athletes. In: *Proceedings of the 24th international symposium on biomechanics in sports*, Salzburg, 14–18 July 2006.
[21] Lin, CT, Kuo, KP, Hsieh, H, et al. The novel biomechanical measurement and analysis system for tug-of-war. In: *Proceedings of the 34th international symposium on biomechanics in sports*, Tsukuba, Japan, 18–22 July 2016.
[22] Godfrey, M, Nakagawa, M, and Yamamoto, H. Team pulling technique of the tug of war-a birds-eye analysis of tow. In: *Proceedings of the 25th international symposium on biomechanics in sports*, Ouro Preto, Brazil, 23–27 August 2007.
[23] Kawahara, S, Hosaka, M, Cao, Y, et al. Biomechanical considerations of pulling force in tug of war with computer simulation. In: *Proceedings of the 19th international symposium on biomechanics in sports*, Ouro Preto, Brazil, 23–27 August 2001.
[24] Zhang, W, Du, X, and Zhao, Z. Mechanical analysis of tug-of-war games 1. *Mech Eng* 2021; 43(2): 313.
[25] Zhang, B. Parametric analysis in tug-of-war based on ideal biomechanical model. *Appl Mech Mater* 2012; 192: 207–210.
[26] Moulton, DE, Lessinnes, TH, and Goriely, A. Morphoelastic rods. Part I: a single growing elastic rod. *J Mech Phys Solids* 2013; 61(2): 398–427.
[27] Goriely, A. *The mathematics and mechanics of biological growth*, *Interdisciplinary applied mathematics*, vol. 45. 1st ed. New York: Springer, 2017.
[28] Kaczmarski, B, Moulton, DE, Kuhl, E, et al. Active filaments I: Curvature and torsion generation. *J Mech Phys Solids* 2022; 164: 104918.
[29] Goriely, A, Moulton, DE, and Angela Mihai, L. A rod theory for liquid crystalline elastomers. *J Elast* 2022; 153: 509–532.
[30] Johnson, KL. *Contact mechanics*. Cambridge: Cambridge University Press, 1987.
[31] McGinnis, PM. *Biomechanics of sport and exercise*. Harrogate: Human Kinetics, 2013.

[32] Bartlett, R. *Introduction to sports biomechanics: analysing human movement patterns*. Abingdon: Routledge, 2014.
[33] Blazevich, A. *Sports biomechanics: the basics: optimising human performance*. London: Bloomsbury Publishing, 2017.
[34] Baca, A. Mathematical modelling in sport and human movement science. *Math Comput Model Dyn Syst* 2017; 23(4): 361–362.
[35] Gernigon, C, Briki, W, and Eykens, K. The dynamics of psychological momentum in sport: the role of ongoing history of performance patterns. *J Sport Exerc Psychol* 2010; 32(3): 377–400.
[36] Song, K, Zou, Q, and Shi, J. Modelling the scores and performance statistics of NBA basketball games. *Commun Stat Simul Comput* 2020; 49(10): 2604–2616.
[37] Vračar, P, Štrumbelj, E, and Kononenko, I. Modeling basketball play-by-play data. *Expert Syst Appl* 2016; 44: 58–66.

Appendix 1

On material parameters

In this appendix, we outline the rationale for the material parameters used in the model.

On stiffness parameters. Both the arms and the legs satisfy a constitutive law of the form

$$n = K(\alpha - 1), \tag{31}$$

where n is the resultant force, α is the "elastic" stretch/compression, and K is the longitudinal stiffness. It is important to note that in our modelling framework, K does not correspond to the actual material stiffness of an arm or leg, which in principle could be measured in terms of the material stiffnesses of the constitutive parts (muscle, bone, tissue, ...). Rather, K characterises the strength of the arms/legs taken as a pair. To obtain a reasonable value for this parameter, we consider the force-generating abilities of the player. For the legs, this will be connected to how much weight the player can lift, for example, in a squat lift. Suppose the player is in a squat position holding a mass M above their shoulders, where M is the maximum weight the player is able to hold and return to an upright position. In the morphoelastic framework, we idealise this lift by saying that when the player is in the squat position, they have $\alpha_i^L < 1$, and they return to the standing position by activating the leg muscles, $\gamma_i^L > 1$, such that the position ends with $\gamma_i^L = 1/\alpha_i^L$. The world record for squat lift is just under 500 kg, though the average person can squat only around 120 kg. Supposing that the addition of the mass M, without any leg activation, causes the player to bend to a squat position, $\alpha^L \approx 2/3$, we would have $K^L \approx -Mg/(\alpha^L - 1) = 3Mg$. Taking $M = 100$ kg gives a value of $K^L = 3000$ N.

A similar thought experiment could be used to estimate the stiffness for the arms, though as leg muscles will generally be much stronger than arm muscles, we have used a baseline value $K_i^A = 500$ N.

We also require rotational stiffness values for the upper and lower body. For the lower body, the terms κ_i^L in the torque components $\kappa_i^L(\theta_i - \hat{\theta}_i)$ of equation (2) and (5) characterise the ability of the legs to resist a rotation of the lower body, that is, a change in stance. This stiffness constant again depends on the strength in the legs, though only one leg: the front leg alone can resist a rotation forward, while only the back leg can resist a rotation backwards. We may thus estimate this value as close to half of the stiffness K^L, multiplied by the length of the lower body. This gives a value in the range of 500–1500 Nm; in our simulations, we have used $\kappa^L = 1000$ Nm. For the upper body, the parameter κ^T in the torque component $\kappa^L\phi$ of equation (3) describes the strength of the upper body to resist rotation at the hips. This will depend on abdominal muscles and core strength. We have used a value $\kappa^T\phi = 800$ Nm, similar to κ^L but a bit smaller.

On concentrated mass. For computational simplicity, we have concentrated the mass of each player in the upper torso. A simple calculation suggests how much of a decreased mass one should consider when compared to a distributed mass. Suppose that an elastic rod has length L and total mass M. The resultant force n in the body will satisfy $n'(S) = \rho g$, where S is the reference arc length and ρ is the linear density, satisfying $\rho = M/L$ in the case of uniformly distributed mass [26]. If $S = 0$ corresponds to the base of the body, and $S = L$ is the top, then $n(L) = 0$ (the top is stress-free), and thus $n = \rho g(S - L)$. Letting α denote the elastic compression due to self-weight and suppose α satisfies a linear law $n = K(\alpha - 1)$, where as before K is the stiffness. If s is the arc length of the body deformed under self-weight, then $\alpha = \mathrm{d}s/\mathrm{d}S$, and thus the height of the deformed body satisfies

$$\ell = \int_0^L \alpha(S)\,\mathrm{d}S = L + \int_0^L \frac{n(S)}{E}\,\mathrm{d}S. \tag{32}$$

Inserting the form for n and integrating, we obtain

$$\ell = L\left(1 - \frac{Mg}{2K}\right). \tag{33}$$

Suppose instead that a mass $\widehat{M}$ is concentrated at the top of the body, $S = L$, what value should $\widehat{M}$ take in order to best mimic the more realistic distributed mass? In the case of concentrated mass, the resultant force n is constant and equal to $-\widehat{M}g$. Taking the same constitutive law, $n = k(\alpha - 1)$, and performing the same calculation for ℓ as above, we obtain

$$\ell = L\left(1 - \frac{\widehat{M}g}{K}\right). \tag{34}$$

Therefore, the deformed lengths are equivalent if $\widehat{M} = M/2$. Note that this choice also produces equivalent torques. That is, consider the torque about the contact point with the ground of a rigid body of length L with constant density (mass per length) ρ, and total mass M making an angle θ with the horizontal. The torque about the contact point with the ground, due to self-weight, is

$$T = \int_0^L \rho g(s\cos\theta, s\sin\theta, 0)^T \times (-\mathbf{e}_y)\, ds \tag{35}$$

which simplifies to $-Mg\cos\theta L/2$ using the connection $M = \rho L$. A concentrated mass $\widehat{M}$ located at $s = L$, on the contrary, produces a torque $\widehat{T} = -\widehat{M}g\cos\theta L$, and thus $\widehat{T} = T$ if $\widehat{M} = M/2$. In our simulations, we have thus used $m_i = 40$ kg as baseline values, corresponding to 80 kg players.

On dynamic coefficients. The dynamic equations require moments of inertia for balance of angular momentum and drag coefficients. To obtain an estimate for the moment of inertia, we suppose that the mass $M = 40$ kg is distributed through a rectangular cylinder of dimensions ($w = 0.18$ m) $\times$ ($d = 0.1$ m) $\times$ ($h = 0.8$ m) (a very rough approximation of the lower body of a human). Aligning the x-axis with the width and the z-axis with the depth, the relevant moment of inertia corresponds to rotation about the z-axis and is given by

$$\mathcal{I}^L = \int_0^h \int_0^w \int_0^d \rho(x^2 + y^2)\, \mathrm{d}x\mathrm{d}y\mathrm{d}z, \tag{36}$$

where $\rho = M/V$, $V = dwh$ being the total volume. This calculation gives $\mathcal{I}^L \approx 4.8$ kg m^2; we have used $\mathcal{I}_i^L = \mathcal{I}_i^T = 5$ kg m^2 in our simulations.

The drag coefficients are more difficult to estimate accurately. However, it seems clear that in a game of tug of war, oscillations will be over-damped or very nearly over-damped. The values we have used came from numerical experimentation.